5.74 Introductory Quantum Mechanics II
Spring 2009

10.2. <u>DIAGRAMMATIC PERTURBATION THEORY</u>

In practice, the nonlinear response functions as written above provide little insight into what the molecular origin of particular nonlinear signals is. These multiply nested terms are difficult to understand when faced the numerous light-matter interactions, which can take on huge range of permutations when performing experiments on a system with multiple quantum states. The different terms in the response function can lead to an array of different nonlinear signals that vary not only microscopically by the time-evolution of the molecular system, but also differ macroscopically in terms of the frequency and wavevector of the emitted radiation.

Diagrammatic perturbation theory (DPT) is a simplified way of keeping track of the contributions to a particular nonlinear signal given a particular set of states in H_0 that are probed in an experiment. It uses a series of simple diagrams to represent the evolution of the density matrix for H_0, showing repeated interaction of ρ with the fields followed by time-propagation under H_0. From a practical sense, DPT allows us to interpret the microscopic origin of a signal with a particular frequency and wavevector of detection, given the specifics of the quantum system we are studying and the details of the incident radiation. It provides a shorthand form of the correlation functions contributing to a particular nonlinear signal, which can be used to understand the microscopic information content of particular experiments. It is also a bookkeeping method that allows us to keep track of the contributions of the incident fields to the frequency and wavevector of the nonlinear polarization.

There are two types of diagrams we will discuss, Feynman and ladder diagrams, each of which has certain advantages and disadvantages. For both types of diagrams, the first step in drawing a diagram is to identify the states of H_0 that will be interrogated by the light-fields. The diagrams show an explicit series of absorption or stimulated emission events induced by the incident fields which appear as action of the dipole operator on the *bra* or *ket* side of the density matrix. They also symbolize the coherence or population state in which the density matrix evolves during a given time interval. The trace taken at the end following the action of the final dipole operator, i.e. the signal emission, is represented by a final wavy line connecting dipole coupled states.

Feynman Diagrams[1]

Feynman diagrams are the easiest way of tracking the state of coherences in different time periods, and for noting absorption and emission events.

1. Double line represents *ket* and *bra* side of ρ.
2. Time-evolution is upward.
3. Lines intersecting diagram represent field interaction. Absorption is designated through an inward pointing arrow. Emission is an outward pointing arrow. Action on the left line is action on the *ket*, whereas the right line is *bra*.
4. System evolves freely under H_0 between interactions, and density matrix element for that period is often explicitly written.
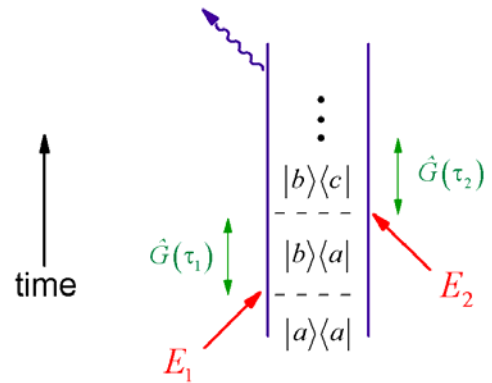
Ladder Diagrams[2]

Ladder diagrams are helpful for describing experiments on multistate systems and/or with multiple frequencies; however, it is difficult to immediately see the state of the system during a given time interval. They naturally lend themselves to a description of interactions in terms of the eigenstates of H_0.

1. Multiple states arranged vertically by energy.
2. Time propagates to right.
3. Arrows connecting levels indicate resonant interactions. Absorption is an upward arrow and emission is downward. A solid line is used to indicate action on the *ket*, whereas a dotted line is action on the *bra*.
4. Free propagation under H_0 between interactions, but the state of the density matrix is not always obvious.
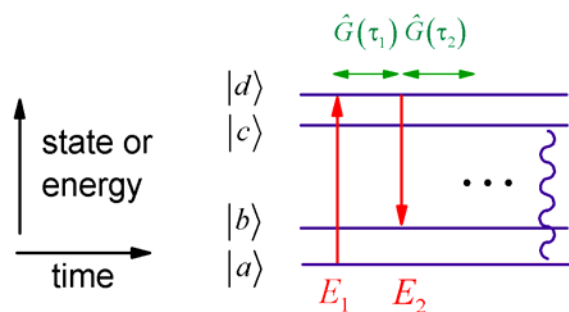
For each light-matter interactions represented in a diagram, there is an understanding of how this action contributes to the response function and the final nonlinear polarization state. Each light-matter interaction acts on one side of ρ, either through absorption or stimulated emission. Each interaction adds a dipole matrix element μ_{ij} that describes the interaction amplitude and any orientational effects.[3] Each interaction adds input electric field factors to the polarization, which are used to describe the frequency and wavevector of the radiated signal. The action of the final dipole operator must return you to a diagonal element to contribute to the signal. Remember that action on the *bra* is the complex conjugate of *ket* and absorption is complex conjugate of stimulated emission. A table summarizing these interactions contributing to a diagram is below.

Interaction	Diagrammatic Representation	contrib. to $R^{(n)}$	contribution to $\mathbf{k}_{sig}$ & ω_{sig}	
KET SIDE				
Absorption $\left(\bar{\mu}_{ba}\cdot\bar{E}_n\right)\exp\left[i\bar{k}_n\cdot\bar{r}-i\omega_n t\right]$		$\bar{\mu}_{ba}\cdot\hat{\varepsilon}_n$	$+\mathbf{k_n}$	$+\omega_n$
Stimulated Emission $\left(\bar{\mu}_{ba}\cdot\bar{E}_n^*\right)\exp\left[-i\bar{k}_n\cdot\bar{r}+i\omega_n t\right]$		$\bar{\mu}_{ba}\cdot\hat{\varepsilon}_n$	$-\mathbf{k_n}$	$-\omega_n$
BRA SIDE				
Absorption $\left(\bar{\mu}_{ba}^*\cdot\bar{E}_n^*\right)exp\left[-i\bar{k}_n\cdot\bar{r}+i\omega_n t\right]$		$\bar{\mu}_{ba}^*\cdot\hat{\varepsilon}_n$	$-\mathbf{k_n}$	$-\omega_n$
Stimulated Emission $\left(\bar{\mu}_{ba}^*\cdot\bar{E}_n\right)exp\left[i\bar{k}_n\cdot\bar{r}-i\omega_n t\right]$		$\bar{\mu}_{ba}^*\cdot\hat{\varepsilon}_n$	$+\mathbf{k_n}$	$+\omega_n$
SIGNAL EMISSION: (Final trace, convention: ket side)		$\bar{\mu}_{ba}\cdot\hat{\varepsilon}_{an}$		

Once you have written down the relevant diagrams, being careful to identify all permutations of interactions of your system states with the fields relevant to your signal, the correlation functions contributing to the material response and the frequency and wavevector of the signal field can be readily obtained. It is convenient to write the correlation function as a product of several factors for each event during the series of interactions:

1) Start with a factor p_n signifying the probability of occupying the initial state, typically a Boltzmann factor.

2) Read off products of transition dipole moments for interactions with the incident fields, and for the final signal emission.

3) Multiply by terms that describe the propagation under H_0 between interactions.

   As a starting point for understanding an experiment, it is valuable to include the effects of relaxation of the system eigenstates in the time-evolution using a simple phenomenological approach. Coherences and populations are propagated by assigning the damping constant Γ_{ab} to propagation of the ρ_{ab} element:

$$\hat{G}(\tau)\rho_{ab} = \exp[-i\omega_{ab}\tau - \Gamma_{ab}\tau]\rho_{ab}. \tag{10.1}$$

   Note $\Gamma_{ab} = \Gamma_{ba}$ and $G_{ab}^* = G_{ba}$. We can then recognize $\Gamma_{ii}=1/T_1$ as the population relaxation rate for state i and $\Gamma_{ij} = 1/T_2$ the dephasing rate for the coherence ρ_{ij}.

4) Multiply by a factor of $(-1)^n$ where n is the number of *bra* side interactions. This factor accounts for the fact that in evaluating the nested commutator, some correlation functions are subtracted from others.

5) The radiated signal will have frequency $\omega_{sig} = \sum_i \omega_i$ and wave vector $\bar{k}_{sig} = \sum_i \bar{k}_i$

Example: Linear Response for a Two-Level System

Let's consider the diagrammatic approach to the linear absorption problem, using a two-level system with a lower level a and upper level b. There is only one independent correlation function in the linear response function,

$$C(t) = Tr\left[\mu(t)\mu(0)\rho_{eq}\right]$$
$$= Tr\left[\mu\,\hat{G}(t)\mu\,\rho_{eq}\right]$$

(10.2)

This does not need to be known before starting, but is useful to consider, since it should be recovered in the end. The system will be taken to start in the ground state ρ_{aa}. Linear response only allows for one input field interaction, which must be absorption, and which we take to be a *ket* side interaction. We can now draw two diagrams:

(4) Act on *ket* with μ and take trace.

(3) Propagate under H_0:
$$G_{ab}(\tau) = e^{-i\omega_{ba}\tau - \Gamma_{ba}\tau}.$$

(2) Act on ket with $\mu(0)$ to create ρ_{ba}.

(1) Start in ρ_{aa} (add factor of p_a when reading).
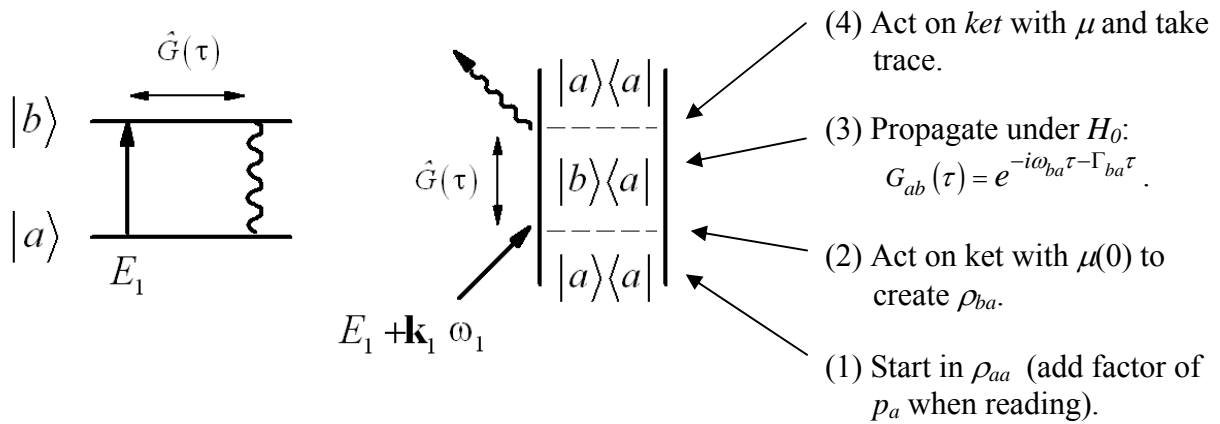
With this diagram, we can begin by describing the signal characteristics in terms of the induced polarization. The product of incident fields indicates:

$$E_1\,e^{-i\omega_1 t + i\bar{k}_1\cdot\bar{r}} \quad \Rightarrow \quad P(t)e^{-i\omega_{sig}t + i\bar{k}_{sig}\cdot\bar{r}}$$

(10.3)

so that
$$\omega_{sig} = \omega_1 \quad \bar{k}_{sig} = \bar{k}.$$

(10.4)

As expected the signal will radiate with the same frequency and in the same direction as the incoming beam. Next we can write down the correlation function for this term. Working from bottom up:

$$\overset{\text{(1) (2)}}{} \quad \overset{\text{(3)}}{} \quad \overset{\text{(4)}}{}$$
$$C(t) = p_a\left[\mu_{ba}\right]\left[e^{-i\omega_{ba}t - \Gamma_{ba}t}\right]\left[\mu_{ab}\right]$$
$$= p_a\left|\mu_{ba}\right|^2 e^{-i\omega_{ba}t - \Gamma_{ba}t}$$

(10.5)

More sophisticated ways of treating the time-evolution under H_0 in step (*3*) could take the form of some of our earlier treatments of the absorption lineshape:

$$\hat{G}(\tau)\rho_{ab} \sim \rho_{ab}\exp\left[-i\omega_{ab}\tau\right]F(\tau)$$
$$= \rho_{ab}\exp\left[-i\omega_{ab}\tau - g(t)\right]$$

(10.6)

Note that one could draw four possible permutations of the linear diagram when considering *bra* and *ket* side interactions, and initial population in states *a* and *b*:
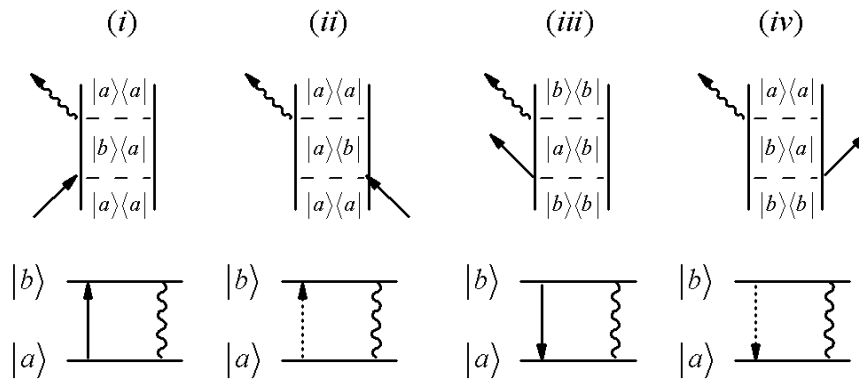
However, there is no new dynamical content in these extra diagrams, and they are generally taken to be understood through one diagram. Diagram *ii* is just the complex conjugate of eq. (10.5) so adding this signal contribution gives:

$$C(t) - C^*(t) = 2i\,p_a\left|\mu_{ba}\right|^2\sin(\omega_{ba}t)e^{-\Gamma_{ba}t}.$$

(10.7)

Accounting for the thermally excited population initially in *b* leads to the expected two-level system response function that depends on the population difference

$$R(t) = \frac{2}{\hbar}(p_a - p_b)\left|\mu_{ba}\right|^2\sin(\omega_{ba}t)e^{-\Gamma_{ba}t}.$$

(10.8)

Example: Second-Order Response for a Three-Level System

The second-order response is the simplest nonlinear case, but in molecular spectroscopy is less commonly used than third-order measurements. The signal generation requires a lack of inversion symmetry, which makes it useful for studies of interfaces and chiral systems. However, let's show how one would diagrammatically evaluate the second order response for a very specific system pictured at right. If we only have population in the ground state at equilibrium and if there are only resonant interactions allowed, the permutations of unique diagrams are as follows:

$|c\rangle$ —— E_c

$|b\rangle$ —— E_b

$|a\rangle$ —— E_a

$$\frac{Q_1}{ket\,/\,ket} \qquad\qquad\qquad \frac{Q_2}{bra/ket}$$

(i)	(ii)	(iii)	(iv)

$$k_{sig} = k_1 + k_2 \qquad\quad k_1 - k_2 \qquad\qquad -k_1 + k_2 \qquad\qquad -k_1 + k_2$$

$$\omega_{sig} = \omega_1 + \omega_2 \qquad \omega_1 - \omega_2 \qquad\qquad -\omega_1 + \omega_2 \qquad\quad -\omega_1 + \omega_2$$

$$= \omega_{ba} + \omega_{cb} = \omega_{ca} \qquad \omega_{ca} + \omega_{bc} = \omega_{ba} \qquad -\omega_{ba} + \omega_{ca} = \omega_{cb} \qquad -\omega_{ca} + \omega_{ba} = \omega_{bc}$$
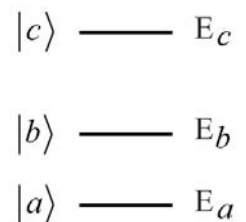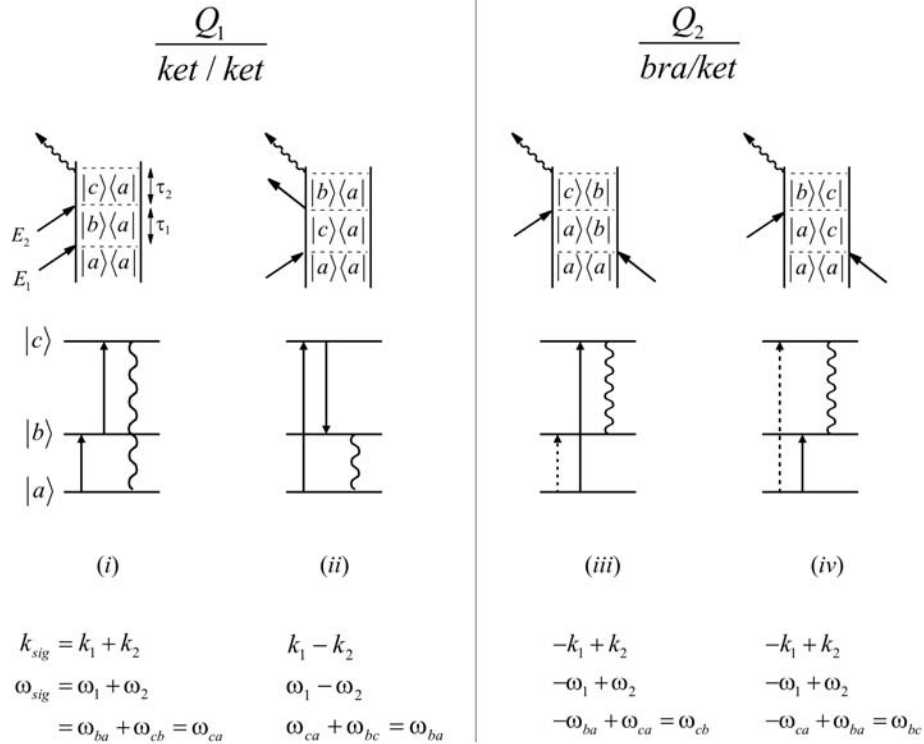
From the frequency conservation conditions, it should be clear that process *i* is a sum-frequency signal for the incident fields, whereas diagrams *ii-iv* refer to difference frequency schemes. To better interpret what these diagrams refer to let's look at *iii*. Reading in a time-ordered manner, we can write the correlation function corresponding to this diagram as

$$
\begin{aligned}
C_2 &= Tr\left[\mu(\tau)\rho_{eq}\mu(0) \right] \\
&= (-1)^1 \mu_{bc}\,\hat{G}_{cb}(\tau_2)\,\mu_{ca}\,\hat{G}_{ab}(\tau_1)\,\rho_{aa}\,\mu_{ba}^* \, . \\
&= -p_a\mu_{ab}\mu_{bc}\mu_{ca}e^{-i\omega_{ab}\tau_1-\Gamma_{ab}\tau_1}e^{-i\omega_{cb}\tau_2-\Gamma_{cb}\tau_2}
\end{aligned}
\tag{10.9}
$$

Note that a literal interpretation of the final trace in diagram *iv* would imply an absorption event – an upward transition from *b* to *c*. What does this have to do with radiating a signal? On the one hand it is important to remember that a diagram is just mathematical shorthand, and that one can't distinguish absorption and emission in the final action of the dipole operator prior to taking a trace. The other thing to remember is that such a diagram always has a complex conjugate associated with it in the response function. The complex conjugate of *iv*, a Q_2^* *ket/bra* term, shown at right has a downward transition –emission– as the final interaction. The combination $Q_2 - Q_2^*$ ultimately describes the observable.

$$\frac{Q_2^*}{ket/bra}$$

$(iv)^*$
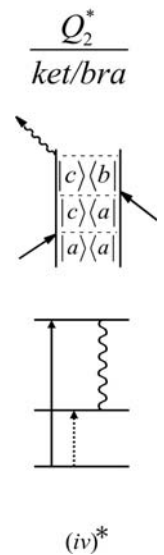
Now, consider the wavevector matching conditions for the second order signal *iii*. Remembering that the magnitude of the wavevector is $\left|\bar{k}\right| = \omega/c = 2\pi/\lambda$, the length of the vectors will be scaled by the resonance frequencies. When the two incident fields are crossed as a slight angle, the signal would be phase-matched such that the signal is radiated closest to beam 2. Note that the most efficient wavevector matching here would be when fields 1 and 2 are collinear.
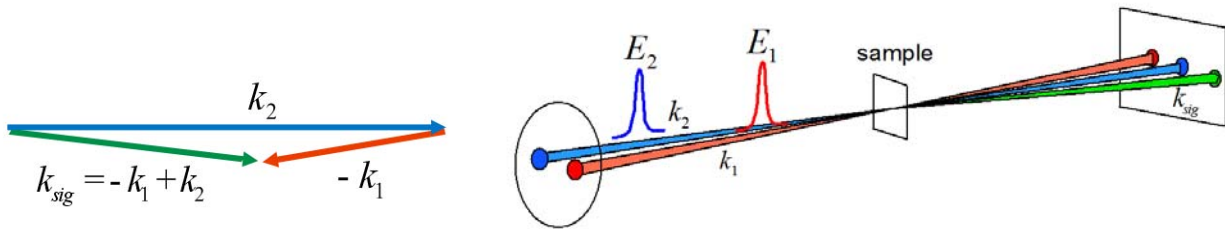
Third-Order Nonlinear Spectroscopy

Now let's look at examples of diagrammatic perturbation theory applied to third-order nonlinear spectroscopy. Third-order nonlinearities describe the majority of coherent nonlinear experiments that are used including pump-probe experiments, transient gratings, photon echoes, coherent anti-Stokes Raman spectroscopy (CARS), and degenerate four wave mixing (4WM). These experiments are described by some or all of the eight correlation functions contributing to $R^{(3)}$:

$$R^{(3)} = \left(\frac{i}{\hbar}\right)^3 \sum_{\alpha=1}^{4} \left[R_\alpha - R_\alpha^*\right] \tag{10.10}$$

The diagrams and corresponding response first requires that we specify the system eigenstates. The simplest case, which allows us discuss a number of examples of third-order spectroscopy is a two-level system. Let's write out the diagrams and correlation functions for a two-level system starting in ρ_{aa}, where the dipole operator couples $|b\rangle$ and $|a\rangle$.

R_1	R_2	R_3	R_4
ket/ket/ket	bra/ket/bra	bra/bra/ket	ket/bra/bra

$$+\omega_1 - \omega_2 + \omega_3$$
$$k_{sig} = +k_1 - k_2 + k_3$$

$$-\omega_1 + \omega_2 + \omega_3$$
$$-k_1 + k_2 + k_3$$

$$-\omega_1 + \omega_2 + \omega_3$$
$$-k_1 + k_2 + k_3$$

$$+\omega_1 - \omega_2 + \omega_3$$
$$+k_1 - k_2 + k_3$$
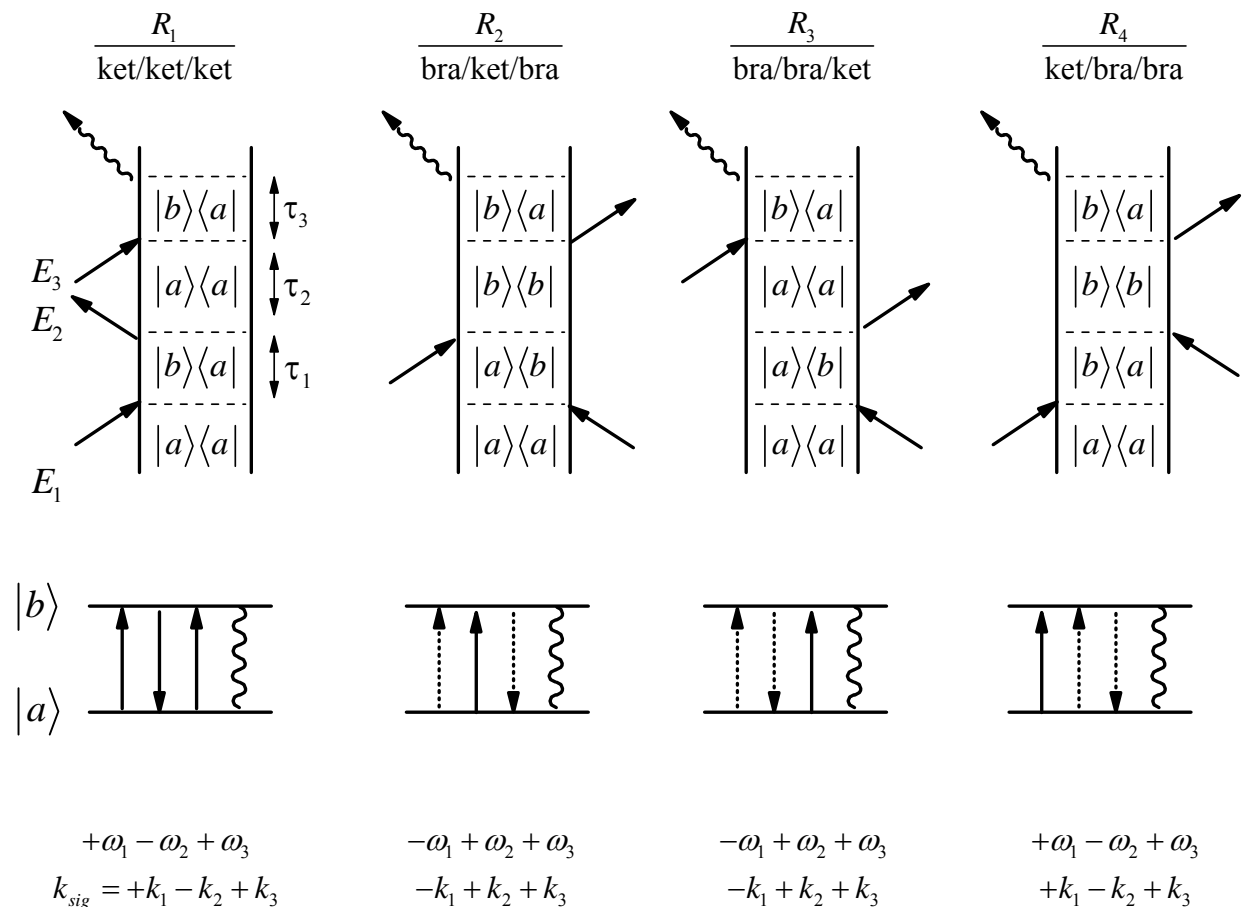
As an example, let's write out the correlation function for R_2 obtained from the diagram above. This term is important for understanding photon echo experiments and contributes to pump-probe and degenerate four-wave mixing experiments.

$$R_2 = (-1)^2 \, p_a \left(\mu_{ba}^* \right) \left[e^{-i\omega_{ab}\tau_1 - \Gamma_{ab}\tau_1} \right] (\mu_{ba}) \left(e^{-i\omega_{bb}\tau_2 - \Gamma_{bb}\tau_2} \right) (\mu_{ab}^*) \left[e^{-i\omega_{ba}\tau_3 - \Gamma_{ba}\tau_3} \right] (\mu_{ab})$$
$$= p_a \left| \mu_{ab} \right|^4 \exp \left[-i\omega_{ba} (\tau_3 - \tau_1) - \Gamma_{ba} (\tau_1 + \tau_3) - \Gamma_{bb} (\tau_2) \right]$$

(10.11)

The diagrams show how the input field contributions dictate the signal field frequency and wave-vector. Recognizing the dependence of $E_{sig}^{(3)} \sim P^{(3)} \sim R_2 (E_1 E_2 E_3)$, these are obtained from the product of the incident field contributions

$$\bar{E}_1 \bar{E}_2 \bar{E}_3 = \left(E_1^* \, e^{+i\omega_1 t - i\bar{k}_1 \cdot \bar{r}} \right) \left(E_2 \, e^{-i\omega_2 t + i\bar{k}_2 \cdot r} \right) \left(E_3 \, e^{+i\omega_3 t - i\bar{k}_3 \cdot \bar{r}_3} \right)$$
$$\Rightarrow E_1^* E_2 \, E_3 \, e^{-\omega_{sig} t + i\bar{k}_{sig} \cdot \bar{r}}$$

(10.12)

$$\therefore \quad \omega_{sig 2} = -\omega_1 + \omega_2 + \omega_3$$
$$k_{sig 2} = -\bar{k}_1 + \bar{k}_2 + \bar{k}_3$$

(10.13)

Now, let's compare this to the response obtained from R_4. These we obtain

$$R_4 = p_a \left| \mu_{ab} \right|^4 \exp \left[-i\omega_{ba} (\tau_3 + \tau_1) - \Gamma_{ba} (\tau_1 + \tau_3) - \Gamma_{bb} (\tau_2) \right]$$

(10.14)

$$\omega_{sig 4} = +\omega_1 - \omega_2 + \omega_3$$
$$k_{sig 4} = +\bar{k}_1 - \bar{k}_2 + \bar{k}_3$$

(10.15)

Note that R_2 and R_4 terms are identical, except for the phase acquired during the initial period: $\exp[i\phi] = \exp[\pm i\omega_{ba}\tau_1]$. The R_2 term evolves in conjugate coherences during the τ_1 and τ_3 periods, whereas the R_4 term evolves in the same coherence state during both periods:

	Coherences in τ_1 and τ_3	Phase acquired in τ_1 and τ_3
R_4	$\|b\rangle\langle a\| \rightarrow \|b\rangle\langle a\|$	$e^{-i\omega_{ba}(\tau_1 + \tau_3)}$
R_2	$\|a\rangle\langle b\| \rightarrow \|b\rangle\langle a\|$	$e^{-i\omega_{ba}(\tau_1 - \tau_3)}$

The R_2 term has the property of time-reversal: the phase acquired during τ_1 is reversed in τ_3. For that reason the term is called "rephasing." Rephasing signals are selected in photon echo experiments and are used to distinguish line broadening mechanisms and study spectral diffusion. For R_4, the phase acquired continuously in τ_1 and τ_3, and this term is called "non-

rephasing." Analysis of R_1 and R_3 reveals that these terms are non-rephasing and rephasing, respectively.
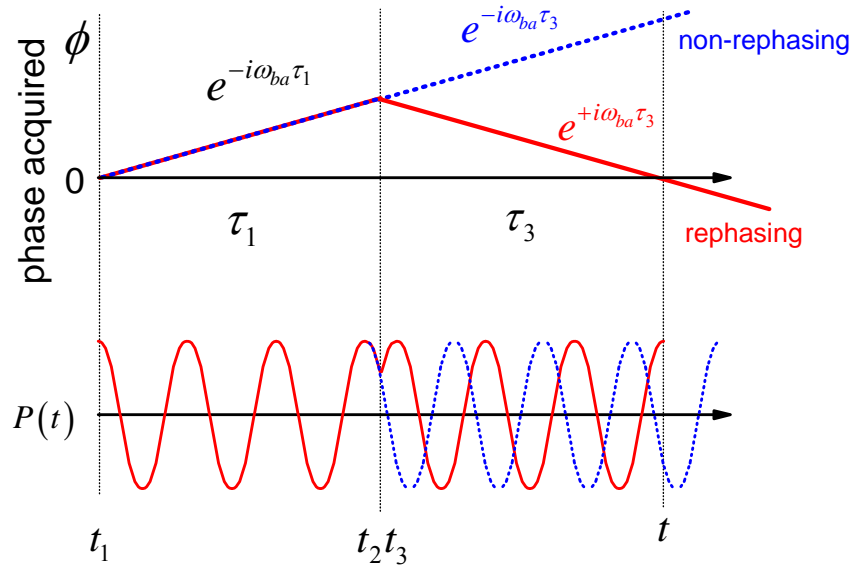
For the present case of a third-order spectroscopy applied to a two-level system, we observe that the two rephasing functions R_2 and R_3 have the same emission frequency and wavevector, and would therefore both contribute equally to a given detection geometry. The two terms differ in which population state they propagate during the τ_2 variable. Similarly, the non-rephasing functions R_1 and R_4 each have the same emission frequency and wavevector, but differ by the τ_2 population. For transitions between more than two system states, these terms could be separated by frequency or wavevector (see appendix). Since the rephasing pair R_2 and R_3 both contribute equally to a signal scattered in the $-k_1 + k_2 + k_3$ direction, they are also referred to as S_I. The nonrephasing pair R_1 and R_4 both scatter in the $+k_1 - k_2 + k_3$ direction and are labeled as S_{II}.

Our findings for the four independent correlation functions are summarized below.

			ω_{sig}	k_{sig}	τ_2 population
S_I	rephasing	R_2	$-\omega_1 + \omega_2 + \omega_3$	$-k_1 + k_2 + k_3$	excited state
		R_3	$-\omega_1 + \omega_2 + \omega_3$	$-k_1 + k_2 + k_3$	ground state
S_{II}	non-rephasing	R_1	$+\omega_1 - \omega_2 + \omega_3$	$+k_1 - k_2 + k_3$	ground state
		R_4	$+\omega_1 - \omega_2 + \omega_3$	$+k_1 - k_2 + k_3$	excited state

Frequency Domain Representation[4]

A Fourier-Laplace transform of $P^{(3)}(t)$ with respect to the time intervals allows us to obtain an expression for the third order nonlinear susceptibility, $\chi^{(3)}(\omega_1, \omega_2, \omega_3)$:

$$P^{(3)}(\omega_{sig}) = \chi^{(3)}(\omega_{sig}; \omega_1, \omega_2, \omega_3) \bar{E}_1 \bar{E}_2 \bar{E}_3 \tag{10.16}$$

where
$$\chi^{(n)} = \int_0^\infty d\tau_n \, e^{i\Omega_n \tau_n} \cdots \int_0^\infty d\tau_1 \, e^{i\Omega_1 \tau_1} \, R^{(n)}(\tau_1, \tau_2, \dots \tau_n) \, . \tag{10.17}$$

Here the Fourier transform conjugate variables Ω_m to the time-interval τ_m are the sum over all frequencies for the incident field interactions up to the period for which you are evolving:

$$\Omega_m = \sum_{i=1}^m \omega_i \tag{10.18}$$

For instance, the conjugate variable for the third time-interval of a $+k_1 - k_2 + k_3$ experiment is the sum over the three preceding incident frequencies $\Omega_3 = \omega_1 - \omega_2 + \omega_3$.

In general, $\chi^{(3)}$ is a sum over many correlation functions and includes a sum over states:

$$\chi^{(3)}(\omega_1, \omega_2, \omega_3) = \frac{1}{6}\left(\frac{i}{\hbar}\right)^3 \sum_{abcd} p_a \sum_{\alpha=1}^4 \left[\chi_\alpha - \chi_\alpha^*\right] \tag{10.19}$$

Here a is the initial state and the sum is over all possible intermediate states. Also, to describe frequency domain experiments, we have to permute over all possible time orderings. Most generally, the eight terms in $R^{(3)}$ lead to 48 terms for $\chi^{(3)}$, as a result of the 3!=6 permutations of the time-ordering of the input fields.[5]

Given a set of diagrams, we can write the nonlinear susceptibility directly as follows:

1) Read off products of light-matter interaction factors.

2) Multiply by resonance denominator terms that describe the propagation under H_0. In the frequency domain, if we apply eq. (10.17) to response functions that use phenomenological time-propagators of the form eq. (10.1), we obtain

$$\hat{G}(\tau_m)\rho_{ab} \Rightarrow \frac{1}{(\Omega_m - \omega_{ba}) - i\Gamma_{ba}} \, . \tag{10.20}$$

Ω_m is defined in eq. (10.18).

3) As for the time domain, multiply by a factor of $(-1)^n$ for n bra side interactions.

4) The radiated signal will have frequency $\omega_{sig} = \sum_i \omega_i$ and wavevector $\bar{k}_{sig} = \sum_i \bar{k}_i$.

As an example, consider the term for R_2 applied to a two-level system that we wrote in the time domain in eq. (10.11)

$$
\begin{aligned}
\chi_2 &= |\mu_{ba}|^4 \frac{(-1)}{\omega_{ab}-(-\omega_1)-i\Gamma_{ab}} \cdot \frac{1}{\cancel{\omega_{bb}}-(\omega_2-\omega_1)-i\Gamma_{bb}} \cdot \frac{(-1)}{\omega_{ba}-(\omega_3+\omega_2-\omega_1)-i\Gamma_{ba}} \\
&= |\mu_{ba}|^4 \frac{1}{\omega_1-\omega_{ba}-i\Gamma_{ba}} \cdot \frac{1}{-(\omega_2-\omega_1)-i\Gamma_{bb}} \cdot \frac{1}{-(\omega_3+\omega_2-\omega_1-\omega_{ba})-i\Gamma_{ba}}
\end{aligned}
\tag{10.21}
$$

The terms are written from a diagram with each interaction and propagation adding a resonant denominator term (here reading left to right). The full frequency domain response is a sum over multiple terms like these.

Appendix: Third-order diagrams for a four-level system

The third order response function can describe interaction with up to four eigenstates of the system Hamiltonian. These are examples of correlation functions within $R^{(3)}$ for a four-level system representative of vibronic transitions accompanying an electronic excitation, as relevant to resonance Raman spectroscopy. Note that these diagrams present only one example of multiple permutations that must be considered given a particular time-sequence of incident fields that may have variable frequency.

$\underline{R_1}$	$\underline{R_2}$	$\underline{R_3}$	$\underline{R_4}$
ket / ket / ket	*bra/ket/bra*	*bra/bra/ket*	*ket/bra/bra*

$$\mu_{ba}\mu_{cb}\mu_{dc}\mu_{ad} \qquad \mu_{ba}^{*}\mu_{da}\mu_{cb}^{*}\mu_{cd} \qquad \mu_{ba}^{*}\mu_{cb}^{*}\mu_{da}\mu_{cd} \qquad \mu_{ba}\mu_{da}^{*}\mu_{cd}^{*}\mu_{cb}$$

$$\omega_{sig} = +\omega_1 - \omega_2 + \omega_3 \qquad -\omega_1 + \omega_2 + \omega_3 \qquad -\omega_1 + \omega_2 + \omega_3 \qquad +\omega_1 - \omega_2 + \omega_3$$

$$= \omega_{ba} + \omega_{cb} + \omega_{dc} = \omega_{da} \quad -\omega_{ba} + \omega_{da} - \omega_{cb} = \omega_{dc} \quad -\omega_{ba} - \omega_{cb} + \omega_{da} = \omega_{dc} \quad \omega_{ba} - \omega_{da} - \omega_{cd} = \omega_{bc}$$
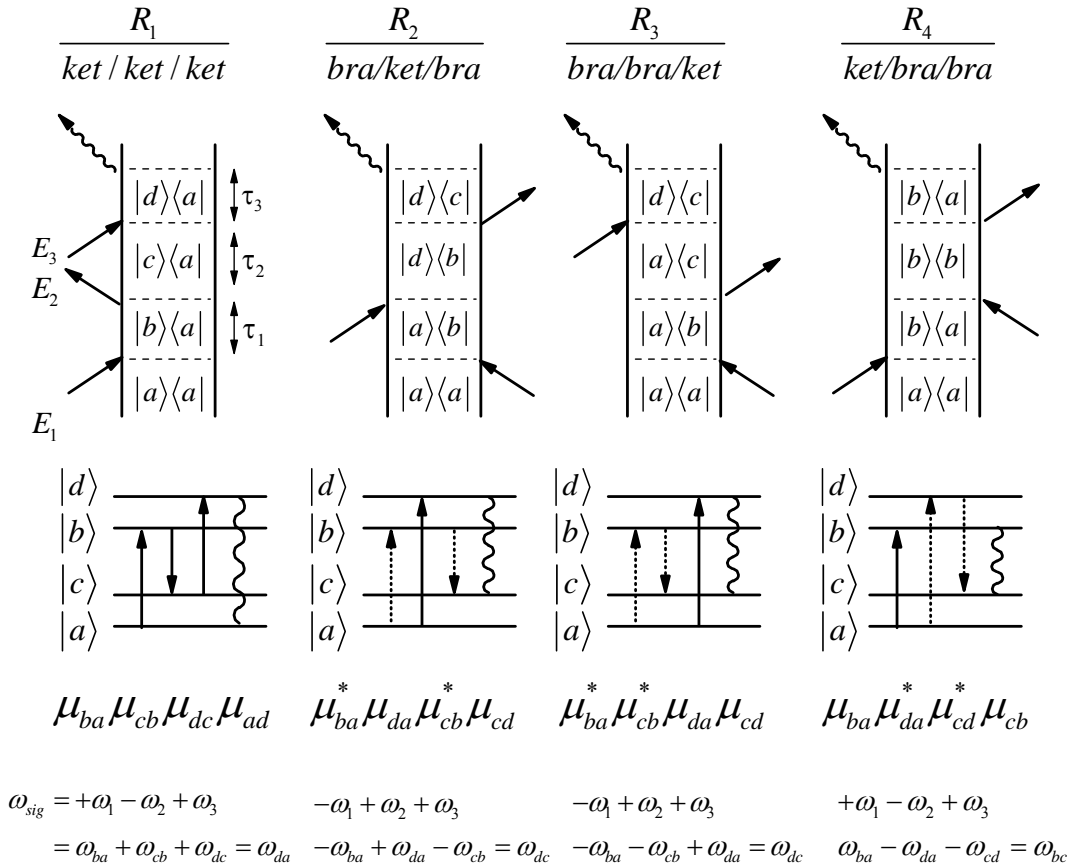
The signal frequency comes from summing all incident resonance frequencies accounting for the sign of the excitation. The products of transition matrix elements are written in a time-ordered fashion without the projection onto the incident field polarization needed to properly account for orientational effects. The R_1 term is more properly written $\left\langle \left(\overline{\mu}_{ba} \cdot \hat{\varepsilon}_1 \right) \left(\overline{\mu}_{cb} \cdot \hat{\varepsilon}_2 \right) \left(\overline{\mu}_{dc} \cdot \hat{\varepsilon}_3 \right) \left(\overline{\mu}_{ad} \cdot \hat{\varepsilon}_{an} \right) \right\rangle$.

Note that the product of transition dipole matrix elements obtained from the sequence of interactions can always be re-written in the cyclically invariant form $\mu_{ab}\mu_{bc}\mu_{cd}\mu_{da}$. This is one further manifestation of closed loops formed by the sequence of interactions.

Appendix: Third-order diagrams for a vibration

The third-order nonlinear response functions for infrared vibrational spectroscopy are often applied to a weakly anharmonic vibration. For high frequency vibrations in which only the $v = 0$ state is initially populated, when the incident fields are resonant with the fundamental vibrational transition, we generally consider diagrams involving the system eigenstates $v = 0$, 1 and 2, and which include v=0-1 and v=1-2 resonances. Then, there are three distinct signal contributions:

Signal	k_{sig}	Diagrams and Transition Dipole Scaling			R/NR
S_I	$-k_1 + k_2 + k_3$	$\lvert \mu_{10} \rvert^4$	$\lvert \mu_{10} \rvert^4$	$\lvert \mu_{10} \rvert^2 \lvert \mu_{21} \rvert^2$	rephasing
S_{II}	$+k_1 - k_2 + k_3$	$\lvert \mu_{10} \rvert^4$	$\lvert \mu_{10} \rvert^4$	$\lvert \mu_{10} \rvert^2 \lvert \mu_{21} \rvert^2$	non-rephasing
S_{III}	$+k_1 + k_2 - k_3$	$\lvert \mu_{10} \rvert^2 \lvert \mu_{21} \rvert^2$	$\lvert \mu_{10} \rvert^2 \lvert \mu_{21} \rvert^2$		non-rephasing

Note that for the S_I and S_{II} signals there are two types of contributions: two diagrams in which all interactions are with the v=0-1 transition (fundamental) and one diagram in which there are two interactions with v=0-1 and two with v=1-2 (the overtone). These two types of contributions have opposite signs, which can be seen by counting the number of *bra* side interactions, and have emission frequencies of ω_{10} or ω_{21}. Therefore, for harmonic oscillators, which have $\omega_{10} = \omega_{21}$ and $\sqrt{2}\mu_{10} = \mu_{21}$, we can see that the signal contributions should destructively interfere and vanish. This is a manifestation of the finding that harmonic systems display no nonlinear response. Some deviation from harmonic behavior is required to observe a signal, such as vibrational anharmonicity $\omega_{10} \neq \omega_{21}$, electrical anharmonicity $\sqrt{2}\mu_{10} \neq \mu_{21}$, or level-dependent damping $\Gamma_{10} \neq \Gamma_{21}$ or $\Gamma_{00} \neq \Gamma_{11}$.

1 . Yee, T. K. & Gustafson, T. K. Diagrammatic analysis of the density operator for nonlinear optical calculation: Pulsed and cw responses. *Phys. Rev. A* **18**, 1597 (1978)

Fujimoto, J.G. and Yee, T.K., Diagrammatic Density Matrix Theory of Transient Four-Wave Mixing and the Measurement of Transient Phenomena. *IEEE J. Quantum Electron.* **QE-22,** 1215 (1986)

Druet, S. A. J., Taran, J.-P. E. & Bordé, C. J. Line shape and Doppler broadening in resonant CARS and related nonlinear processes through a diagrammatic approach. *J. Phys.* **40**, 819 (1979).

Mukamel, S. *Principles of Nonlinear Optical Spectroscopy* (Oxford University Press, New York, 1995).

Shen, Y. R. *The Principles of Nonlinear Optics* (Wiley-Interscience, New York, 1984).

2. D. Lee and A. C. Albrecht, "A unified view of Raman, resonance Raman, and fluorescence spectroscopy (and their analogues in two-photon absorption)." Adv. Infrared and Raman Spectr. **12**, 179 (1985).

3. To properly account for all orientational factors, the transition dipole moment must be projected onto the incident electric field polarization $\hat{\varepsilon}$ leading to the terms in the table. This leads to a nonlinear polarization that can have *x, y,* and *z* polarization components in the lab frame. The are obtained by projecting the matrix element prior to the final trace onto the desired analyzer axis $\hat{\varepsilon}_{an}$.

4. Prior, Y. A complete expression for the third order susceptibility $\chi^{(3)}$ -perturbative and diagramatic approaches. *IEEE J. Quantum Electron.* **QE-20**, 37 (1984).

See also, Dick, B. Response functions and susceptibilities for multiresonant nonlinear optical spectroscopy: Perturbative computer algebra solution including feeding. *Chem. Phys.* **171**, 59 (1993).

5. Bloembergen, N., Lotem, H. & Lynch, R. T. Lineshapes in coherent resonant Raman scattering. *Indian J. Pure Appl. Phys.* **16**, 151 (1978).